

Porous Anodic Alumina with Continuously Manipulated Pore/Cell Size

Wei Chen, Jian-Shuang Wu, and Xing-Hua Xia*

Key Laboratory of Analytical Chemistry for Life Science, School of Chemistry and Chemical Engineering, Nanjing University, Nanjing 210093, China

Nanoporous anodic alumina, which has been widely used as anticorrosion or decoration coating to improve the mechanical properties of aluminum,¹ is now attracting renewed attention as an indispensable part of the nanoscience and nanotechnology.² The porous anodic alumina (PAA) films possess uniform cylindrical pore sizes and high pore density, which are known to be important membrane attributes. These nanosized pores can serve as perfect scaffold platform for synthesizing nanostructural arrays of various materials.^{3–8} Furthermore, nanoporous alumina membranes are suitable for a number of diverse applications, including DNA translocation, size-exclusive filtration, gas separation, and as photonic crystal.^{9–12}

These versatile applications are due to the special physical characteristics of the porous anodic alumina, which can be fabricated through the relatively simple and low-cost anodization process. When a sheet of aluminum is electrochemically anodized in a certain acid electrolyte under specific conditions, an almost perfectly regular ordered porous alumina film with controlled pore size and thickness forms on a thin barrier layer alumina (BLA) covered aluminum substrate.^{13–16}

To expand the application field and optimize the effectiveness of the porous anodic alumina, it is essential to improve the regularity of the pores' arrangement, and to manipulate the size and position of the pores. For instance, the mass transport property, which is important in the application of PAA as a separation membrane, is strongly dependent on the pore diameter. Potential utilization of PAA in membrane separation requires precise control of the pore diameter. For these purposes, a variety of investigations concerning the mor-

ABSTRACT We used polyethyleneglycol (PEG) as a modulator to manipulate pore and cell sizes in the porous anodic alumina (PAA) fabrication. It is shown for the first time that continuous manipulation of the pore size of PAA can be realized. Combined with the coexistent cell-size controlling effect, the morphology and properties of this important nanoscale template and separation membrane can be precisely regulated. The pore size modulation mechanism is proposed on the basis of the morphological and electrochemical results. The presence of PEG in the electrolyte results in a more compacted structure of the barrier layer alumina (BLA), although the barrier layer thickness does not change considerably. In addition, the additive can obviously restrain the chemical dissolution of alumina and shape smaller pores. These two effects combined with the increased viscosity of the electrolyte slow down the ion transportation and diminish the anodization current. Thus, the burning-down phenomena of the aluminum substrates can be avoided at relatively high voltage anodization, and an interpore distance up to 610 nm can be achieved.

KEYWORDS: porous anodic alumina · anodization · morphology control · polyethyleneglycol · phosphoric acid

phology control have been extensively performed after the confirmation of the classical cell model proposed by Keller *et al.*¹⁷ An extensive series of experiments by O'Sullivan and Wood showed conclusively that the barrier layer thickness, pore diameter, and the interpore spacing all increase nearly linearly with the voltage of the electrochemical cell and decrease with increasing acid strength of the electrolyte.¹⁸ Films of controlled morphology can be possibly developed by fine-tuning the acid used, the pH of the electrolyte, the temperature, the anodization voltage, and the current density. To achieve highly ordered PAA films, a two-step anodization process and a pretexturing process were proposed by Masuda and co-workers.^{3,19} Recently, most research work in this aspect has been primarily concentrating on the formation procedures in oxalic acid and sulfuric acid.^{20,21} But few attentions have been paid on the relatively hardly controlled phosphoric acid system. Moreover, these studies were only focusing on the interpore diameter modulation;

*Address correspondence to xhxia@nju.edu.cn.

Received for review November 28, 2007 and accepted March 31, 2008.

Published online April 18, 2008.
10.1021/nn700389j CCC: \$40.75

© 2008 American Chemical Society

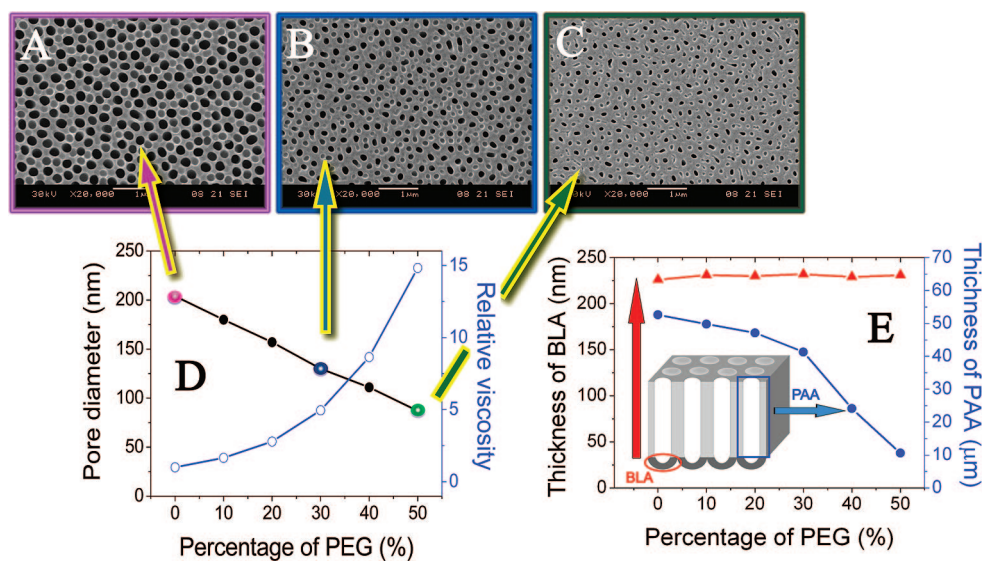


Figure 1. Influence of the PEG addition on the morphology of alumina films electrochemically grown in 0.2 M H_3PO_4 at 165 V and 15 °C. The outer surface SEM images of the film formed with (A) 0% PEG, (B) 30% PEG, and (C) 50% PEG; (D) dependence of the pore diameter on the PEG proportion in the electrolyte; (E) dependence of the PAA and BLA thickness on the PEG proportion in the electrolyte.

the pore diameter was seldom a concern, although it is also an important parameter in the PAA applications.

As it is generally believed that the formation voltage significantly determines the pore morphology, anodization performed at as high a voltage as possible could result in a relatively larger cell. Practically, many authors have suggested that this goal can only be achieved by anodizing the aluminum in a phosphoric acid solution but not in other acidic solutions.²² However, a major limitation associated with this electrolyte type is its aggressiveness, which results in the serious chemical dissolution of pore walls that thus promotes the enlargement of the pore openings. In addition, the uppermost issue of high voltage anodization is the avoidance of breakdown or burning of the oxide film caused by catastrophic flow of electric current.

To obtain PAA with adjustable pore size and constant interpore distance, we used polyethyleneglycol (PEG, MW 400) as a modulator in the anodization process in a phosphoric acid solution. It was found that the pore opening effect could be significantly restrained. By changing the concentration ratio of PEG to phosphoric acid, the pore size of the PAA membrane fabricated at constant voltages can be tuned at will. Furthermore, the addition of PEG decreases the anodizing current, which suppresses the breakdown effect and enables the uniform growth of the oxide films at high voltages (>200 V). Therefore, the fabrication voltage can be extended to 230 V at near room temperature in a 0.2 M phosphoric acid electrolyte, and the interpore distance can be increased to 610 nm which is *ca.* 100 nm larger than that reported previously. This information provides us with the ability to tailor-make membranes with a range of characteristics that can be used for a number of different experimental studies and practical applications.

RESULTS AND DISCUSSION

The surface morphology images of the PAA membranes fabricated in a 0.2 M phosphoric acid electrolyte with different concentration of PEG are shown in Figure 1. The size of pores opening decreases significantly by the addition of PEG and is inversely proportional to the content of PEG in the electrolyte. The pore size manipulation may be due to two effects caused by the PEG addition. First, as reported previously by Ono and co-workers,²³ the ratio of pore to cell diameter (or interpore distance) is controlled by the electric field strength during anodizing. This ratio decreases with the increase of electric field strength. Generally, the electric field strength is inversely proportional to the dielectric coefficient of the electrolyte. Since the dielectric coefficient of PEG is lower than that of water, the addition of PEG could cause the increase of the electric field strength. It is assumed that the film with a low pore-to-cell diameter ratio would be formed with the increase of electric field strength because of the addition of PEG. Thus, the pore size controlling mechanism is assumed to be partially related to the high electric field strength during the anodic film growth in the presence of PEG. Another effect which may play a prior role in the pore size dwindling is the protecting effect of PEG on the chemical dissolution process. It is generally accepted that the pores generally broaden toward the film surface owing to the chemical dissolution of pore walls by electrolyte during the film growth.²⁴ The reduced diameter of the pore opening in the presence of PEG could be explained by the decreased chemical dissolution reaction rate. To verify this hypothesis, the PAA films were immersed in a fresh phosphoric acid solution for 4 h after anodization. The total amount of the aluminum cations dissolved in the electrolyte was

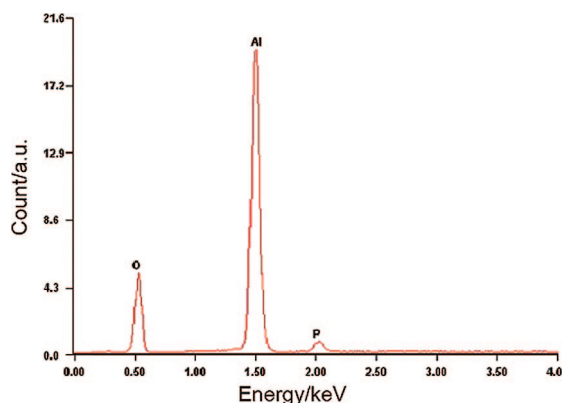


Figure 2. Energy dispersive X-ray (EDX) spectrum of porous anodic alumina film formed in 0.2 M phosphoric acid containing 75% PEG at 165 V and 15 °C.

determined by spectrophotometry. The chemical dissolution rate was calculated to be 0.625 and 2.5 mg/h in the presence and absence of 50% PEG, respectively. This implies that the presence of PEG could obviously decrease the chemical dissolution rate of alumina in phosphoric acid solution.

The thickness of the porous anodic alumina and the barrier oxide layers was measured by SEM characterization. The PEG concentration dependent thickness of the PAA films and the corresponding barrier layers anodized under the same conditions is shown in Figure 1E. It is well-known for alumina that the barrier layer thickness is linearly proportional to the applied potential, which guarantees that no new pores nucleate between existing pores.²⁵ It is clear that the thickness of the barrier layer keeps the same in the PEG concentration ranging from 0% to 50%. The growth parameter of the barrier layers formed during the anodization of aluminum is usually quoted in term of anodizing rate (the number of nanometers of oxide layer formed per Volt applied). With the knowledge of the oxide film thickness and the voltage applied, the anodizing ratio can be approximately calculated. It is about 1.4 nm/V under our experimental conditions, which is in good consistency with the expectation of the voltage dependence reported in ref 1. In contrast, the PAA film thickness decreases with the increase of PEG concentration. This could be explained by the formation mechanism which will be discussed in the latter section.

The energy dispersive X-ray (EDX) spectrum of the PAA film formed in the phosphoric acid solution containing 75% PEG reveals that the alumina film is mainly composed of Al (K_{α} , 1.5 keV) and O (K_{α} , 0.525 keV) (Figure 2). A small peak for P is observed at 2.0 keV, indicating a small amount of phosphate anion incorporated into the PAA film during the anodizing process. This is good agreement with the classical PAA formation mechanism. From the spectrum, we can also infer that PEG is not incorporated into the PAA film because no X-ray emission peak for C was observed. In addition, elemental and thermalgravimetric analysis was also car-

ried out to confirm the EDX result. There is no carbon or hydrogen detected by the elemental analysis, and no PEG weight loss step exists in the thermalgravimetric characterization (see Supporting Information, Figure S1). These results imply that the variation in morphology of PAA films formed in the presence of PEG cannot be ascribed to the chemical composition.

As studied in the previous works, the formation process in the constant-voltage mode is accompanied by a high initial current for the formation of the insulating barrier oxide film. With the increase of the insulating layer thickness, a steep current decrease occurs. This current then increases because of the formation of pores and finally reaches a constant value in the regime of steady-state pore growth.²⁶ The variation of the anodizing current–time curves during constant-voltage anodizing in phosphoric acid solutions containing various concentrations of PEG is shown in Figure 3A. The initial current decrease associated with the formation of a continuous barrier oxide proceeds much slower in the case of PEG addition, which means that it takes a longer time to form a barrier oxide layer of homogeneous thickness. The lowest current, which implies the beginning of the pore initiation, was reached within 30 s when anodization was performed in pure phosphoric acid solution. However, this initial pore nucleation was notably delayed in the presence of PEG, indicating a slow pore initiation. AFM images of the PAA film at the different stages of the anodization were collected to confirm this effect (Figure 3B). In the absence of PEG, a barrier oxide layer starts to grow immediately after switching on the anodic bias. Within 2 s, relatively fine-featured pathways are revealed in the outer regions of the barrier layer prior to any true pore formation. It suggests that the pore nucleation takes place almost at the same time as the barrier layer growth. Further anodization (*e.g.*, for 50 s) results in the propagation of individual paths through the barrier oxide layer and the formation of a steady-state pore structure. In contrast to the conventional anodization process discussed above, the pore formation procedure obviously slowed down when PEG was added into the electrolyte. By anodizing for 2 s, there was an imperceptible change of surface morphology as compared to the aluminum substrate. The morphological variation can be observed only after about 50 and 500 s for pore nucleation and formation, respectively.

It is believed that the steady state anodization current is mainly related to the migration of oxygen-containing ions (O^{2-}/OH^{-}) and Al^{3+} ions in the barrier layer.^{13,26} The mass transport of the oxygen-containing anionic species from the bulk solution to the oxide/metal interface determines the current density during the anodization process. Accordingly, a decreased mass transport rate is expected with the increase of solution viscosity caused by the presence of PEG, which results in the decreased ionic current. Due to the intense agita-

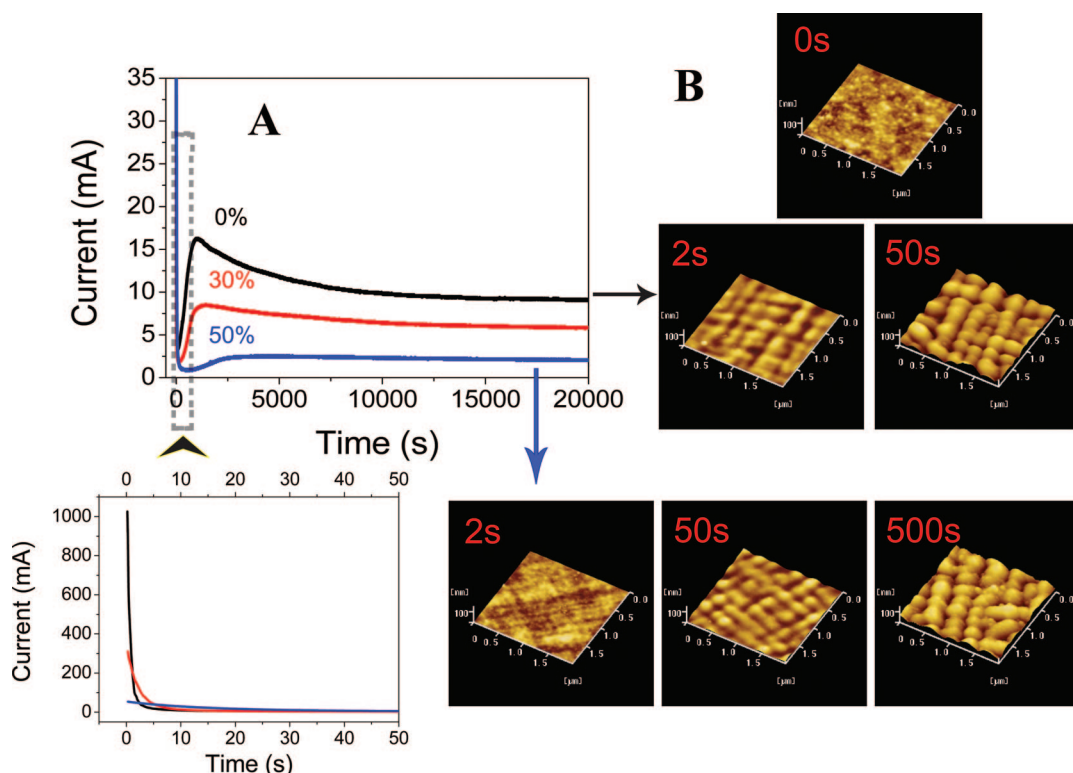


Figure 3. (A) Current–time transients during anodization in a 0.2 M phosphoric acid solution in presence of different PEG proportion at 165 V and 15 °C. (B) AFM images of aluminum substrate after pretreatment of annealing and electropolishing; resultant surface topographies of the aluminum anodizing at 165 V in 0.2 M phosphoric acid in absence of PEG for 2 s, 50 s; and in presence of 50% PEG for 2 s, 50 s, 500 s.

tion, the influence of PEG on the ions migration in the bulk solution can be neglected. However, the influence of solution viscosity on the ions migration rate in the nanopores should be taken into consideration. This effect can be explained in detail by the variation of the electromigration velocity. The electrophoretic velocity (v) of the ions in the nanopores can be described as $v = \epsilon \zeta E / 4 \pi \eta$, where ϵ , ζ , E , and η represent the dielectric coefficient, zeta potential, electric field strength, and the viscosity coefficient, respectively.

All the results reported in the literature show that the ionic current is in directly proportional to the electric field strength in the classical anodization system. But in the present case, the effect of the increasing electric field strength is counteracted by the contribution from the change of dielectric coefficient of the electrolyte. The product of ϵ and E is a constant. Therefore, the ionic current is solely dependent on the viscosity coefficient of the electrolyte.

In addition, two other important factors, the structure of the barrier layer and the pore diameter, should also be considered. In the presence of PEG in the phosphoric acid solution, barrier layer forms slowly at a given anodization voltage. As shown in Figure 1E, the thickness of the barrier layer keeps constant at fixed potential regardless of PEG addition. However, the AC impedance of the barrier layers, which formed in the presence of PEG, increases significantly (Figure 4A). This could imply the formation of a tighter barrier layer

which certainly limits the ion transportation. The electrokinetic measurements of the PAA membrane with a complete barrier layer at a transmembrane potential of 1.0 V in an aluminum sulfate (0.2 M) solution reveal that the ion migration through this anodic film significantly decreases as compared to that formed in the electrolyte without PEG (Figure 4B). This phenomenon might be related to the more compact barrier layer and smaller pores formed in the presence of PEG as well.

The current curves in Figure 3 can also help us to elucidate the influence of PEG on the formation rate of PAA films. According to the classical model, the continuous formation and dissolution of the barrier layer at the base of the pores result in a one-dimensional displacement of this layer into the aluminum substrate. The film thickness is found to increase linearly with time, and the growth rate is found to be dependent on the anodization conditions. The growth rate of PAA film can be estimated by plotting the film thickness as a function of anodization time, where the film thickness is determined from the cross-sectional SEM micrographs. From the time-dependent thickness variations for different PEG concentration, it is found that the growth rate of the PAA film decreases with increasing PEG concentration at a given temperature because of the slower ion transport rate. The formation rate is 6.93 and 1.26 $\mu\text{m}/\text{h}$ for the anodization in the absence and presence of 50% PEG, respectively.

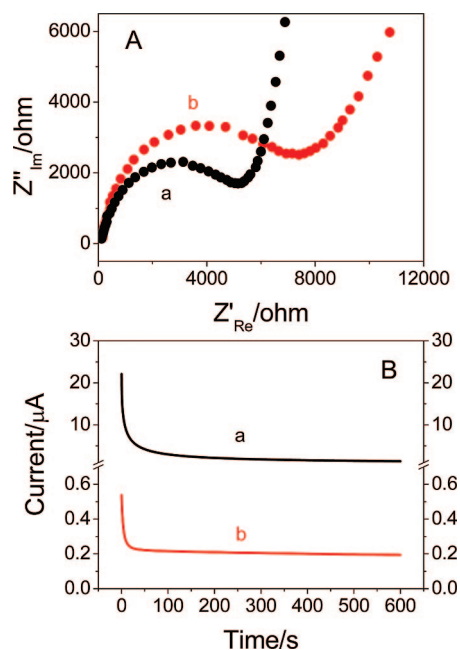


Figure 4. (A) Complex impedance spectra of BLA formed (a) in the absence of PEG and (b) in the presence of 50% PEG at 165 V. (B) Transmembrane current–time curves of the anodic films containing barrier layer formed (a) in the absence of PEG and (b) in the presence of 50% PEG. The transmembrane potential was 1.0 V and the electrolyte was 0.2 M aluminum sulfate.

It is reasonable to assume that the chemical dissolution effect correlates with the anodizing time. On account of slow film growth rate in the presence of PEG, a given thickness should be obtained in longer anodizing time. For instance, a PAA film with thickness of about 55 μm was obtained by 8 h anodization in the absence of PEG, while it required 48 h in the presence of 50% PEG. By anodizing in a long period (48 h), the pore opening is slightly enlarged as compared to the film obtained in the relatively short period (8 h). But it is still much smaller than that of the film formed in the absence of PEG. Another approach to get the given thickness in relatively short time is to increase the concentration of phosphoric acid. Accordingly, both the ionic current and the formation rate of PAA film increase. A PAA film with a thickness of about 55 μm could be formed by 8 h in 0.8 M phosphoric acid solution containing 50% PEG. The pore opening of the resultant film is about 140 nm, which is larger than that formed in 0.2 M phosphoric acid with 50% PEG but still smaller than that formed without PEG. The relationship of the pore opening diameter among the above-mentioned films is shown in Figure 5. The SEM image of the cross section of the PAA film prepared from the phosphoric acid solution containing 50% PEG shows that the size of the pores is uniform throughout the whole film and is the same as that of the pore opening (see Supporting Information, Figure S2). From these results, we can easily fabricate PAA films with the same thickness but with tunable pore size by appropriate design of the

concentration of PEG and phosphoric acid. In addition, control of the pore sizes of PAA films could also be expected by using PEG additives with different molecular weights (MW), as the solution viscosity changes with the polymer MW. For instance, 30% PEG-2000 results in films with 95 nm pores as compared to the film with 130 nm pore size formed in 30% PEG-400 (165 V, 0.2 M H_3PO_4) (see Supporting Information, Figure S3).

It is well known that the anodizing current density increases with the formation voltage. Applied voltages higher than the optimum value required to maintain stable anodization in a given electrolyte always result in “breakdown” or “burning” of the alumina film because of the corrosive acid attack at high electric fields.²³ These process limitations reduce the potential applications of nanoporous alumina. Substantial efforts have been made to explore new self-ordering regimes in a wider range of interpore diameter.^{20,21,23,27} Recently, self-ordering anodization of aluminum has been reported by the Masuda group. Porous alumina film formed in 0.3 M phosphoric acid solution at 195 V and 0 $^\circ\text{C}$ had an almost ideally arranged hexagonal cell configuration with cell size of approximately 500 nm.²⁸ However, in the case of phosphoric acid electrolyte, it is difficult to continue electrolysis for a long time without burning even at a low temperature. The addition of Al^{3+} ions, vigorous agitation, and repeated experiments are suggested to be required to perform relatively stable electrolysis at 195 V for more than 1 h.²³ Our experimental results show that stable anodization in 0.2 M phosphoric acid solution at normal temperature is usually difficult to maintain when the formation voltage exceeds 170 V. In this case, white burning spots appear at the specimen accompanying the high current density and uniform film growth process is terminated. On the basis of the restrain effect of the anodizing current, stable anodization could conceivably be carried out by the addition of PEG in the electrolyte. To obtain PAA film with a higher interpore distance, an anodization voltage of 230 V was applied in the presence of 50% PEG. In this case, breakdown phenomenon did not occur even at a relatively high temperature as compared to that normally used in the high voltage anod-

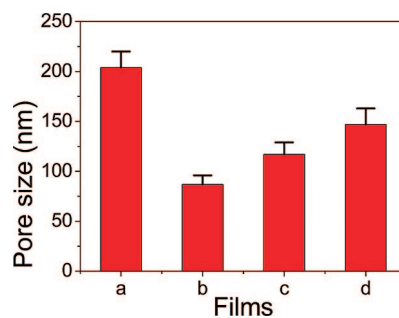


Figure 5. Pore size of the PAA films grown at 165 V and 15 $^\circ\text{C}$. (a) 0.2 M H_3PO_4 for 8 h; (b) 0.2 M H_3PO_4 containing 50% PEG-400 for 8 h; (c) 0.2 M H_3PO_4 containing 50% PEG-400 for 48 h; (d) 0.8 M H_3PO_4 containing 50% PEG-400 for 8 h.

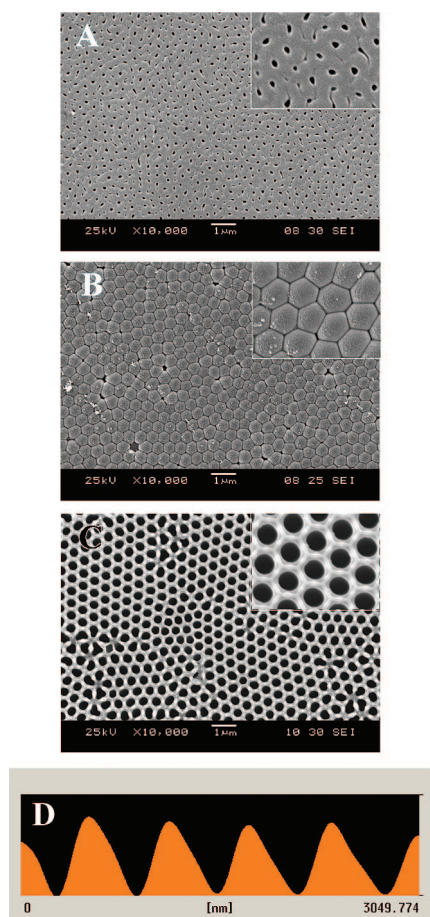


Figure 6. SEM micrographs of anodic porous alumina prepared under a constant voltage condition of 230 V in a 0.2 M H_3PO_4 solution containing 50% PEG at 15 °C for 4 h: (A) surface view; (B) bottom view from the barrier layer; (C) bottom view after pore-widening treatment for 180 min. Panel D shows the AFM height profile of the PAA after pore-widening treatment.

ization, and PAA film with perfect morphology was obtained.

For characterizing the cell configuration from the bottom part of the oxide film, the remaining aluminum was etched in a saturated CuCl_2 solution. The barrier layer was then removed by chemical etching in a 5 wt % aqueous phosphoric acid solution at 45 °C for 180 min to open the pore bottoms. Figure 6 illustrates the typical SEM images of the resultant anodic porous alumina. The pores nucleated on the surface at almost random positions (Figure 6A), which was due to the metallurgical texture of the aluminum substrate.²⁹ The pore diameter is about 70 nm in average from the surface observation. While the surface pore/cell order is poor, the hexagonal ordering toward the metal/oxide interface (Figure 6B) is inherent in the PAA film growth

mechanism.^{13,25} As shown in Figure 6C, a highly ordered pore arrangement with hexagonal texture is achieved within domains that are separated by grain boundaries from neighboring domains with different orientations of pore lattice.

It is well-known for porous anodic alumina that the interpore distance or the cell size, D_{int} ($D_{\text{int}} = kU$), is linearly proportional to the applied cell potential U with a proportionality constant k of approximately 2.5 nm/V. It is predicted by the equation that the D_{int} of the PAA films formed at 230 V should be about 575 nm. As estimated by AFM height profile (Figure 6D), the interpore distance of this film is averaged to be 610 nm. It is consistent with the value of the prediction.

The porosity (P) of the PAA film can be estimated using the equation

$$P = \frac{2\pi}{\sqrt{3}} \left(\frac{D_p}{D_{\text{int}}} \right)^2$$

by assuming an ideal hexagonal arrangement of the pores, where D_p is the pore radius. Although highly ordered and compacted arrays can be obtained under our experimental conditions, the porosity is much smaller than 10% and estimated to be only about 1.6%. This would mean that the 10% porosity rule proposed by Nielsch *et al.* does not hold true in our case,²⁵ where the mechanical stress situated at the metal/oxide interface is different from the conventional process. The decrease in porosity can be ascribed to the weak chemical dissolution under the protection of PEG.

CONCLUSIONS

In summary, an important advantage of the process proposed in this report is that it is possible to tune the pore diameter with constant cell dimension. This template structure provides a natural separation between nanowires or carbon nanotubes after growth, thus preventing the latter to form ropes. By tuning the pore size, the distance between parallel nanoobjects can be facily controlled. Moreover, in contrast to the conventional methods, the strategy employed in this work for the fabrication of PAA film can successfully eliminate the “burning” of alumina film at high anodizing voltages. In phosphoric acid electrolyte, the stable anodization can be carried out at voltages as high as 230 V. In this case, the pore interval extends to 610 nm. On the basis of the identical principle, our approach can also be applied in other acid systems to achieve alumina nanostructures with pore/cell sizes in a large continuous range for various practical applications.

EXPERIMENTAL SECTION

A high purity (99.99%) aluminum sheet was used as the substrate material. Prior to anodizing, it was annealed at 500 °C in nitrogen atmosphere for 5 h in order to remove mechanical

stresses and to recrystallize the samples. Subsequently, the foil was electropolished in a mixture of perchloric acid and ethanol (1:5 by volume) at a constant dc voltage of 20 V for 5 min to smooth the surface. The surface morphology of the aluminum

substrate after pretreatment was evaluated by atomic force microscopy (AFM, SPI-3800N Seiko Japan). The roughness of the electropolished surface was typically between 10 and 20 nm on a lateral length scale of 10 μm . The aluminum foils were then mounted on a copper plate serving as the anode and exposed to the electrolyte in a thermally isolated electrochemical cell. Anodizing process was performed at a constant cell potential condition in a phosphoric acid solution containing various proportions (mass percentage) of PEG (MW 400, Sinopharm Chemical Reagent Company) which was maintained at 15 $^{\circ}\text{C}$ and rigorously stirred. The PEG with MW 400 was used throughout the measurements except otherwise stated. During the anodization, the current–time ($I-t$) curves were recorded to monitor the growth process and compare the influence of PEG on the geometrical structure of the PAA membranes. The surface morphologies of the PAA membranes were characterized using a JSM-6360 LV scanning electron microscope. Thermogravimetric analysis (TGA) was conducted on a Perkin-Elmer TGA-7 instrument. The samples were heated at 20 K min^{-1} from room temperature to 800 $^{\circ}\text{C}$ in nitrogen atmosphere.

Acknowledgment. This work was financially supported by the National Basic Research Program (Grant 2007CB714501), the National Natural Science Foundation of China (Grant 20535010), the National Science Fund for Creative Research Groups (Grant 20521503), and Natural Science Foundation of Fujian Province of China (Grant C0710024).

Supporting Information Available: Thermogravimetric curve and cross-sectional SEM micrograph of PAA film fabricated in the presence of 50% PEG-400; SEM micrograph of PAA prepared in the presence of 30% PEG-2000. This material is available free of charge via the Internet at <http://pubs.acs.org>.

REFERENCES AND NOTES

- Diggle, J. W.; Downie, T. C.; Goulding, C. W. Anodic Oxide Films on Aluminum. *Chem. Rev.* **1969**, *69*, 365–405.
- Asoh, H.; Ono, S. Design of Two-Dimensional/Three-Dimensional Composite Porous Alumina by Colloidal Crystal Templating and Subsequent Anodization. *Appl. Phys. Lett.* **2005**, *87*, 103102.
- Masuda, H.; Fukuda, K. Ordered Metal Nanohole Arrays Made by a Two-Step Replication of Honeycomb Structures of Anodic Alumina. *Science* **1995**, *268*, 1466–1468.
- Lee, S. B.; Mitchell, D. T.; Trofin, L.; Nevanen, T. K.; Soderlund, H.; Martin, C. R. Antibody-Based Bio-Nanotube Membranes for Enantiomeric Drug Separations. *Science* **2002**, *296*, 2198–2200.
- Nielsen, K.; Muller, F.; Li, A. P.; Gosele, U. Uniform Nickel Deposition into Ordered Alumina Pores by Pulsed Electrodeposition. *Adv. Mater.* **2000**, *12*, 582–586.
- Chen, W.; Xia, X. H. An Electrokinetic Method for Rapid Synthesis of Nanotubes. *ChemPhysChem* **2007**, *8*, 1009–1012.
- Masuda, H.; Abe, A.; Nakao, M.; Yokoo, A.; Tamamura, T.; Nishio, K. Ordered Mosaic Nanocomposites in Anodic Porous Alumina. *Adv. Mater.* **2003**, *15*, 161–164.
- Chen, W.; Xia, X. H. Highly Stable Nickel Hexacyanoferrate Nanotubes for Electrically Switched Ion Exchange. *Adv. Funct. Mater.* **2007**, *17*, 2943–2948.
- Rabin, Y.; Tanaka, M. DNA in Nanopores: Counterion Condensation and Coion Depletion. *Phys. Rev. Lett.* **2005**, *94*, 148103.
- Sano, T.; Iguchi, N.; Iida, K.; Sakamoto, T.; Baba, M.; Kawaura, H. Size-Exclusion Chromatography Using Self-Organized Nanopores in Anodic Porous Alumina. *Appl. Phys. Lett.* **2003**, *83*, 4438–4440.
- Lira, H. D. L.; Paterson, R. New and Modified Anodic Alumina Membranes—Part III. Preparation and Characterisation by Gas Diffusion of 5 nm Pore Size Anodic Alumina Membranes. *J. Membr. Sci.* **2002**, *206*, 375–387.
- Masuda, H.; Yamada, M.; Matsumoto, F.; Yokoyama, S.; Mashiko, S.; Nakao, M.; Nishio, K. Lasing from Two-Dimensional Photonic Crystals Using Anodic Porous Alumina. *Adv. Mater.* **2006**, *18*, 213–216.
- Jessensky, O.; Muller, F.; Gosele, U. Self-Organized Formation of Hexagonal Pore Arrays in Anodic Alumina. *Appl. Phys. Lett.* **1998**, *72*, 1173–1175.
- Li, F. Y.; Zhang, L.; Metzger, R. M. On the Growth of Highly Ordered Pores in Anodized Aluminum Oxide. *Chem. Mater.* **1998**, *10*, 2470–2480.
- Li, A. P.; Muller, F.; Birner, A.; Nielsch, K.; Gosele, U. Hexagonal Pore Arrays with a 50–420 nm Interpore Distance Formed by Self-Organization in Anodic Alumina. *J. Appl. Phys.* **1998**, *84*, 6023–6026.
- Chen, W.; Wu, J. S.; Yuan, J. H.; Xia, X. H.; Lin, X. H. An Environment-Friendly Electrochemical Detachment Method for Porous Anodic Alumina. *J. Electroanal. Chem.* **2007**, *600*, 257–264.
- Keller, F.; Hunter, M. S.; Robinson, D. L. Structural Features of Oxide Coatings on Aluminium. *J. Electrochem. Soc.* **1953**, *100*, 411–419.
- O'Sullivan, J. P.; Wood, G. C. The Morphology and Mechanism of Formation of Porous Anodic Films on Aluminium. *Proc. R. Soc. London, Ser. A* **1970**, *317*, 511–543.
- Masuda, H.; Yamada, H.; Satoh, M.; Asoh, H.; Nakao, M.; Tamamura, T. Highly Ordered Nanochannel-Array Architecture in Anodic Alumina. *Appl. Phys. Lett.* **1997**, *71*, 2770–2772.
- Lee, W.; Ji, R.; Gosele, U.; Nielsch, K. Fast Fabrication of Long-Range Ordered Porous Alumina Membranes by Hard Anodization. *Nat. Mater.* **2006**, *5*, 741–747.
- Chu, S. Z.; Wada, K.; Inoue, S.; Isogai, M.; Yasumori, A. Fabrication of Ideally Ordered Nanoporous Alumina Films and Integrated Alumina Nanotubule Arrays by High-Field Anodization. *Adv. Mater.* **2005**, *17*, 2115–2119.
- Jagminas, A.; Bigeliene, D.; Mikulskas, I.; Tomasiunas, R. Growth Peculiarities of Aluminum Anodic Oxide at High Voltages in Diluted Phosphoric Acid. *J. Cryst. Growth* **2001**, *233*, 591–598.
- Ono, S.; Saito, M.; Ishiguro, M.; Asoh, H. Controlling Factor of Self-Ordering of Anodic Porous Alumina. *J. Electrochem. Soc.* **2004**, *151*, B473–B478.
- Patermarakis, G.; Masavetas, K. Aluminium Anodising in Oxalate and Sulphate Solutions. Comparison of Chronopotentiometric and Overall Kinetic Response of Growth Mechanism of Porous Anodic Films. *J. Electroanal. Chem.* **2006**, *588*, 179–189.
- Nielsen, K.; Choi, J.; Schwirn, K.; Wehrspohn, R. B.; Gosele, U. Self-Ordering Regimes of Porous Alumina: The 10% Porosity Rule. *Nano Lett.* **2002**, *2*, 677–680.
- Parkhutik, V. P.; Shershulsky, V. I. Theoretical Modelling of Porous Oxide Growth on Aluminium. *J. Phys. D: Appl. Phys.* **1992**, *25*, 1258–1263.
- Shingubara, S.; Morimoto, K.; Sakaue, H.; Takahagi, T. Self-Organization of a Porous Alumina Nanohole Array Using a Sulfuric/Oxalic Acid Mixture as Electrolyte. *Electrochem. Solid-State Lett.* **2004**, *7*, E15–E17.
- Masuda, H.; Yada, K.; Osaka, A. Self-Ordering of Cell Configuration of Anodic Porous Alumina with Large-Size Pores in Phosphoric Acid Solution. *Jpn. J. Appl. Phys.* **1998**, *37*, L1340–L1342.
- Bocchetta, P.; Sunseri, C.; Masi, R.; Piazza, S.; Di Quarto, F. Influence of Initial Treatments of Aluminium on the Morphological Features of Electrochemically Formed Alumina Membranes. *Mater. Sci. Eng., C* **2003**, *23*, 1021–1026.